Development of a New Method To Evaluate Performance of Accelerator Magnets by Transporting Alpha Particles

Y. Kuriyama*, Y. Mori, KURRI, Osaka, Japan
Y. Kuno, M. Aoki, A. Sato, M. Yoshida, T. Itahashi, Osaka University, Osaka, Japan
Y. Arimoto, KEK, Tsukuba, Japan

Abstract

We are proposing a new method to evaluate accelerator magnets and rings with non-linear dynamics. In this method, a transfer map of higher orders is obtained using the data of particle transportation. The experiment of particle transportation was done. Using the information obtained in the experiment, the transfer map of higher orders with truncated Taylor expansion is calculated.

INTRODUCTION

In designing an accelerator, at first, particle tracking simulation is performed with a magnetic field mapping, which is calculated by a 3-dimensional magnetic field analysis program. After construction of the magnets, real magnetic field distributions of the magnets are measured. The performance of the accelerator is then evaluated by tracking simulation with the measured magnetic field distribution. The accuracy of tracking is limited by either the mesh sizes of the measured field mapping or the precision of measurements. In particular, tracking simulation becomes difficult for a non-linear magnetic field. To avoid these problems, a method of evaluating magnets and their beam-optics performance has been developed, where charged particles from radioactive sources are transported through the magnet. One of the advantages of this method is that any pre-accelerators and injection systems are not required for examining the accelerator magnets, and the evaluation of their accelerator ring can be made with only one accelerator magnet. nother advantage is that the performance of the magnet can be evaluated without any magnetic field measurement.

This method was applied to evaluate the performance of the PRISM-FFAG magnets, for which the details will be described in Section . Because of its large aperture and large magnetic field gradient, non-linearity of a magnetic field is large in case of the PRISM-FFAG magnet. By using these measurements, a transfer map of one cell magnet was obtained. to enable the paper to be reconstructed if there are processing difficulties.

OVERVIEW OF THE PRISM-FFAG MAGNET

PRISM [1] is a next generation muon beam facility, which provides a muon beam with high intensity, high

* kuriyama@rri.kyoto-u.ac.jp

brightness, and high purity. In the PRISM, a FFAG synchrotron [2, 3] is used as a phase rotator of muon and the scaling FFAG has been adopted for the PRISM-FFAG ring [4]. The PRISM-FFAG ring consists of 10 triplet FFAG magnets [5], 8 radio frequency (RF) cavities [6], and 2 kicker magnets. The parameters of the PRISM-FFAG ring are summarized in Table 1.

Table 1: Parameters of the PRISM-FFAG ring.

Parameter	Value
Number of sectors	10
Magnet type	Radial sector, D-F-D
Central Momentum	68 MeV/c
Field index (k)	4.6
F/D ratio	6.2
Opening angle of magnet	F magnet/2 : 2.2 deg
	D magnet : 1.1 deg
Half gap of magnet	17 cm
Average orbit radial	6.4 m
Maximum field	Focus 0.4 T
	Defocus 0.065 T
Tune	Horizontal : 2.73
	Vertical : 1.58

TRUNCATED TAYLOR TRANSFER MAP

The relation between the particle trajectories before and after passing a magnet can be expressed by a transfer map. Suppose a particle has the initial phase-space coordinate $\mathbf{X}(0)$ and is transported to $\mathbf{X}(1)$, the relation between $\mathbf{X}(0)$ and $\mathbf{X}(1)$ can be expressed symbolically using the transfer map M by,

$$\mathbf{X}(1) = M\mathbf{X}(0). \tag{1}$$

Suppose one degree of freedom system, a particle is at a initial phase-space $\mathbf{X(0)} = (X(0), X'(0))$ and a final phase-space $\mathbf{X(1)} = (X(1), X'(1))$. For this case, the linear transfer map is given by

$$X(1) = R_{11}X(0) + R_{12}X'(0), \tag{2}$$
$$X'(1) = R_{21}X(0) + R_{22}X'(0). \tag{3}$$

In order to describe the transfer map of higher orders, truncated Taylor expansions can be used. The transfer map

of higher orders can be given by expanding Eq.(2) with a Taylor expansion as

$$X_a(1) = \sum_b R_{ab} X_b(0) + \sum_{b,c} T_{abc} X_b(0) X_c(0) + \\ \sum_{b,c,d} U_{abcd} X_b(0) X_c(0) X_d(0) + \cdots, \quad (4)$$

where R is the ordinary transfer matrix in the linear matrix theory, T is the second ordered transfer matrix, and U is the third one. Subscripts of a, b, c and d represent the components in phase-space, such as X and X'. This truncated Taylor map will be used in the analysis of this study, as described later.

INTORDUCTION OF SYMPLECTIC CONDITION

The symplectic condition is required by the conservation of Hamiltonian describing a beam. Therefore, the transfer map should be constrained by the symplectic condition. By defining a Jacobian matrix $\mathbf{J}$ of the transfer map M by

$$J_{ab} = \frac{\partial (X(1))_a}{\partial (X(0))_b}, \quad (5)$$

the symplectic condition can be expressed by

$$\mathbf{J^t}(\mathbf{X(0)}) \, \mathbf{S} \, \mathbf{J}(\mathbf{X(0)}) = \mathbf{S} \; for \; all \; \mathbf{X(0)}, \quad (6)$$

where $\mathbf{J^t}$ denotes a transposed matrix of $\mathbf{J}$, and $\mathbf{S}$ is a block matrix expressed as

$$\mathbf{S} = \begin{pmatrix} 0 & \mathbf{I}_n \\ -\mathbf{I}_n & 0 \end{pmatrix}, \quad (7)$$

where $\mathbf{I}_n$ is an n-dimensional unit matrix. To satisfy the condition of Eq.(6), the Jacobian matrix $\mathbf{J}$ should have a unit determinant

$$det\,(\mathbf{J}) = 1. \quad (8)$$

Considering one-dimensional (X, X') system, the Jacobian matrix is expressed by

$$\mathbf{J} = \begin{pmatrix} \dfrac{\partial X(1)}{\partial X(0)} & \dfrac{\partial X(1)}{\partial X'(0)} \\ \dfrac{\partial X'(1)}{\partial X(0)} & \dfrac{\partial X'(1)}{\partial X(0)} \end{pmatrix}. \quad (9)$$

Therefore, the symplectic condition for the linear transfer map is

$$R_{11} R_{22} - R_{12} R_{21} = 1. \quad (10)$$

Although a Taylor expansion cannot be truncated without violating the symplectic condition, the symplectic condition shall be satisfied approximately. When the Taylor transfer expansion is truncated at the second order for one-dimensional (X, X'), the necessary conditions to meet the symplectic requirement in Eq.(8) for all the (X, X') are given by

$$1 = -R_{12} R_{21} + R_{11} R_{22}, \\ 0 = +2R_{22} T_{111} - R_{21} T_{112} - 2R_{12} T_{211} + R_{11} T_{212}, and \quad (11) \\ 0 = +R_{22} T_{112} - 2R_{21} T_{122} - R_{12} T_{212} + 2R_{11} T_{222}.$$

Supposing 2nd order is exact, all of the higher order terms should vanish exactly. The necessary conditions are then

$$0 = -2T_{112} T_{211} + 2T_{111} T_{212}, \\ 0 = -4T_{122} T_{211} + 4T_{111} T_{222}, and \quad (12) \\ 0 = -2T_{122} T_{212} + 2T_{112} T_{222},$$

in addition to Eq.(11).

Table 2 shows two conditions, which are that with and without the symplectic condition. By using the approx-

Table 2: Total numbers of the coefficients necessary for a truncated Taylor transfer map

Map Order	1	2	3	4	5
Without symplectic restriction	4	10	18	28	40
With symplectic restriction	3	7	12	18	25

imate symplectic condition, a total number of the coefficients needed for the truncated Taylor transfer map is reduced.

EXPERIMENTAL APPARATUS

The experiment of transporting alpha particles for the one-cell PRISM-FFAG magnet has been done at the K2 area of the East Counter Hall at KEK. Compared with standard beta ray sources, alpha particle sources have an advantage that its energy is monochromatic. The main components of this experiment are

- the injector [7] and the detector of alpha particle,

- a vacuum system consisting of the injector chamber, the detector chamber, a beam duct, and

- one cell of the PRISM-FFAG magnet.

The injector and detector chambers are located at the both sides of the beam duct. The alpha particle injector and the detector are held inside of these chambers. A schematic view of the setup is shown in Fig. . In Fig. , example particle trajectories are shown in pink lines, and the PRISM-FFAG magnet is shown in green.

Since the PRISM-FFAG ring has 10 cell magnets (namely 10 super-periods), the angle between the two periodic boundaries is 36 degrees. Each super-period is symmetric with respect to the center of super-period. Two independent coordinates were separately defined for the injector and the detector. These two coordinates are symmetric with the respect to the center of magnet. The defined
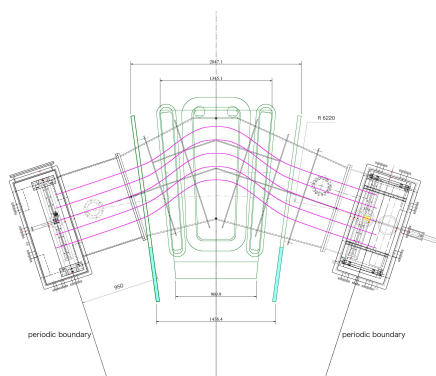
Figure 1: Experimental Setup. The alpha particle injector is on the left-hand side and the alpha particle detector is on the right-hand side. Example particle trajectories are shown in pink lines, and the PRISM-FFAG magnet is shown in green. Two holes located between the magnet and the injection chamber, and also between that and the detection chamber, are those for connecting vacuum pumps.
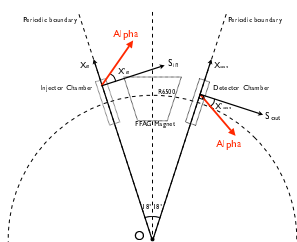

Figure 2: Definition of coordinates

coordinates are shown in Fig. 2. The center of the PRISM-FFAG ring is defined as the origin of a coordinate axis in the radius direction. The lines perpendicular to the periodic boundary is defined as the S_{in} and S_{out} directions. The direction of alpha beam, X'_{in} and X'_{out}, are defined will respect to the S_{in} and S_{out}, respectively.

Alpha Particle Injector

The requirements for the alpha particle injector are high intensity, a small transverse beam sizes, momentum of alpha particles of $\sim$136 MeV/c, and adjustability of the incident positions and angles of alpha particles. To achieve these requirements, the injector consists of

- a specially-ordered standard alpha ray source, ^{241}Am,

- a pair of collimators to determine beam size and directions,

- an energy moderator to adjust the energy of alpha particles, and

- a motorized stage to adjust the positions and angles of alpha particles.

Figure 3 shows a pair of collimators on the moving stage and the specifications of the alpha particle injector are summarized in Table 3.
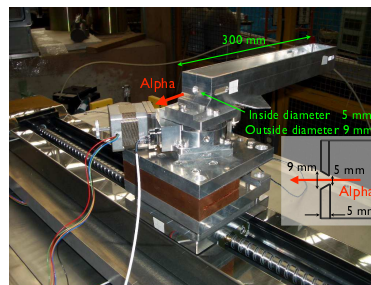

Figure 3: The alpha particle collimators on the moving stage

Table 3: Specifications of the alpha particle injector

Alpha source	^{241}Am 5.486 MeV (85.2%)
Energy moderator	
Material	Aramid film
Thickness	21 μm
Energy loss	2.950 MeV
Average alpha energy	2.536 MeV
FWHM of alpha energy	0.121 MeV
Collimator	
Number of collimators	2
Diameter	5 mm ϕ
Interval	300 mm
Robots	
Stroke	800 mm (radius)
Rotation angle	$\pm$ 45 degrees

Alpha Particle Detector

Because of a low injection rate of the injector, a detection rate of alpha particles is estimated to be less than 1.5 Hz. Since background signals of a few Hz rate is predicted, good particle identification is required. In order to reject backgrounds and measure the positions of the alpha particles, the detector was designed to consist of two kinds of scintillators and multi-anode photomultiplier (MA-PMT). For the purpose of covering large detection region of about 800 mm in horizontal direction, the detector was set up on a motorized moving stage. One of the main backgrounds is beta rays emitted by surrounding materials, such as the windows and inner components of the MA-PMTs. Gamma rays are also background sources. To reject these backgrounds, a combination of ZnS-doped Ag and NE102 (plastic) has been used as a detector. This is a phoswitch-type scintillator detector [8]. ZnS-doped Ag is deposited on acetic-acid-cellulose sheet. The thickness of the acetic-

acid-cellulose sheet was $30 \sim 40 \ \mu$m. To detect alpha particles, a ZnS-sheet was attached onto NE102. The NE102 was glued onto a MA-PMT. Both scintillators, ZnS(Ag) and NE102 were made by OKEN (OHYO KOKEN KOGYO Co. Ltd.). The specifications of the two scintillators are summarized in Table 4.

Table 4: Specifications of the scintillators

Material	ZnS(Ag)	NE102
Thickness	$10 \ \mathrm{mg/cm^2}$	0.5 mm
Decay time	200 ns	2.4 ns
Relative light output		
(as NaI:100)	130	29
Wavelength		
of maximum photon emission	450 nm	423 nm
Index of reflection	2.36	1.58

All the energy of an alpha particle is deposited only in the ZnS-sheet. Therefore, the scintillation light from NE102 is produced by background events, not from alpha particles. Since the decay time of NE102 plastic scintillation-light is quite different from that from a ZnS(Ag), it can identify particles hitting the detector. To discriminate between scintillation light from ZnS(Ag) and NE102, two charge analog digital converters (ADCs) with different gate widths, which are 2 micro-seconds and 200 nano-seconds , were used.

CALCULATION OF TRUNCATED TAYLOR TRANSFER MAP

By using the symplectic condition to the Taylor transfer map, the Taylor transfer map with the 5th order was calculated. In this calculation, a total of 97 different injection positions shown in Fig. 4 were used. This data set taken between August 29 and September 15 in 2007.
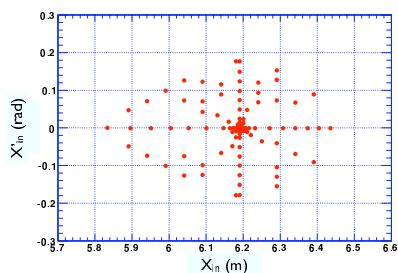

Figure 4: 97 injection points, which are used to calculate higher ordered transfer map.

To calculate the parameters, TMinuit class of ROOT [10] (= Minuit) has been used. Imposing the symplectic condition to the transfer map, the number of fitting parameters is

decreased from 42 to 27, including the parameters for the equilibrium orbit. A calculated chi-square is 200.6 for 167 degrees of freedom.

In the ring coordinate, the equilibrium orbit is given by

$$
\begin{aligned}
X &= 6.1902 \pm 0.0001 \quad \text{m, and} \\
X' &= -0.0007 \pm 0.0001 \ \text{rad.}
\end{aligned}
\tag{13}
$$

Using the linear parts of the transfer map, the betatron tune is given by

$$
\nu_h = 2.734 \pm 0.001
\tag{14}
$$

This value is consistent with the design value of 2.73.

CONCLUSIONS

A new method for evaluating accelerator magnets has been established. In this method, using the information of transporting charged particles through the magnet, the transfer map with the 5th order for one cell has been calculated by imposing an approximate symplectic condition. It is emphasized that the information of transportation is created experimentally.

To realize this method, an alpha particle injector using a standard alpha decay source and the position sensitive alpha particle detector, which is capable of detecting alpha particle in a low counting rate under existing backgrounds, have been developed.

Using the obtained map, the equilibrium orbit and betatron tunes are calculated and in good agreement with the designed values.

REFERENCES

[1] The PRISM project - a muon source of the world highest brightness by phase rotation - Letter of Intent to the J-PARC 50 GeV Proton Synchrotron Experiments, (LoI-24,26)

[2] T. Ohkawa, Symposium on Nuclear Physics of the Physics Society of Japan, private communication (1953).

[3] K. R. Symon *et al.*, Phys. Rev. Sci., Vol.**103**, No.6, p1837 (1956).

[4] A. Sato, Proc. of EPAC'04, p713 (2004).

[5] Y. Arimoto *et al.*, Proc. of Cyclotron Conference 2004, 19p14 (2004).

[6] C. Ohmori *et al.*, Ultra-High Field Gradient RF for Bunch Rotation, Nuclear Physics B - Proceedings Supplements, Volume 149, December 2005, Pages 280-282

[7] S. Araki, Master thesis, Osaka University (2008) in Japanese.

[8] S. Usuda, Nucl. Instr. Meth., A**356**, p334-p338 (1995).

[9] H. Sekiya *et al.*, Nucl. Instr. Meth., A**563**, p49-p53 (2006).

[10] ROOT, An object-oriented analysis framework, http://root.cern.ch.